

Weak Mott insulators on the triangular lattice: Possibility of a gapless nematic quantum spin liquid

Tarun Grover,¹ N. Trivedi,² T. Senthil,¹ and Patrick A. Lee¹

¹*Department of Physics, Massachusetts Institute of Technology, Cambridge, Massachusetts 02139, USA*

²*Department of Physics, Ohio State University, Columbus, Ohio 43210, USA*

(Received 7 March 2010; revised manuscript received 18 May 2010; published 18 June 2010)

We study the energetics of Gutzwiller projected BCS states of various symmetries for the triangular lattice antiferromagnet with a four-particle ring exchange using variational Monte Carlo methods. In a range of parameters the energetically favored state is found to be a projected $d_{x^2-y^2}$ paired state which breaks lattice rotational symmetry. We show that the properties of this nematic or orientationally ordered paired spin-liquid state as a function of temperature and pressure can account for many of the experiments on organic materials. We also study the ring-exchange model with ferromagnetic Heisenberg exchange and find that among the studied ansätze, a projected f -wave state is the most favorable.

DOI: [10.1103/PhysRevB.81.245121](https://doi.org/10.1103/PhysRevB.81.245121)

PACS number(s): 75.10.Jm, 71.27.+a, 74.20.Mn, 74.70.Kn

I. INTRODUCTION

In the last few years the quasi-two-dimensional (2D) organic salts κ -(ET)₂Cu₂(CN)₃ and EtMe₃Sb[Pd(dmit)₂]₂ (abbreviated, respectively, as κ CN and DMIT in the paper) have emerged as possible realizations of Mott insulators in the long sought “quantum spin-liquid” state.^{1–8} These layered materials are believed to be well described by the single band Hubbard model on a nearly isotropic triangular lattice. At ambient pressure they are Mott insulators which do not order magnetically down to temperatures ~ 30 mK (much lower than the exchange $J \sim 250$ K inferred from high-temperature susceptibility).^{1,8} The low-temperature phase is characterized by a linear T -dependent heat capacity and a finite spin susceptibility just like in a metal (even though the material is insulating) (Refs. 1, 4, and 6) indicating the presence of low-lying spin excitations. There is a sharp crossover or possibly a phase transition at a low temperature ≈ 5 K signaled by a peak in the heat capacity and the onset of a drop in the susceptibility.^{1,4} Further an external magnetic field induces inhomogeneity that is evidenced by a broadening of the NMR line.³ Application of moderate pressure (≈ 0.5 GPa) induces a transition to a superconductor (κ CN) or metal (DMIT).²

Broadly speaking a spin-liquid ground state of a Mott insulator cannot be smoothly deformed to the ground state of any electronic band insulator. The theoretical possibility of quantum spin liquids has been appreciated for a long time.⁹ Many sharply distinct spin-liquid phases are possible. Further, any quantum spin-liquid state possesses exotic excitations with fractional quantum number and various associated topological structures. The distinction between different quantum spin-liquid phases is reflected in distinctions of the structure of the low-energy effective theory of these excitations.

Currently the most promising candidate materials all seem to share a few key properties. First, they are weak Mott insulator that are easily driven metallic by application of pressure. Second, they appear to have gapless spin-carrying excitations. We are thus lead to study possible gapless spin-liquid behavior in weak Mott insulators to understand these materials.

At this point, several questions arise: what is a good description of the putative spin-liquid Mott state seen in experiments mentioned above? What is the connection between the superconducting (SC) state and the underlying spin-liquid state that becomes unstable upon applying pressure? What is the nature of the finite-temperature transitions/crossovers? We find, using a variational Monte Carlo analysis of the energetics of several possible wave functions for a spin Hamiltonian with Heisenberg and ring-exchange interactions that the nodal d -wave projected BCS state is the best candidate for the spin liquid. This state has gapless spin excitations and can naturally explain many of the experiments in κ CN though a number of open questions remain. We also study the antiferromagnetic J_4 , ferromagnetic J_2 model, and find that among the studied ansätze, a projected f -wave state is most favorable. This may have bearing on the explanation of the observed gapless spin-liquid behavior in He-3 films.¹²

A. Summary of results

Our results are based on the model Hamiltonian,¹⁰

$$H = 2J_2 \sum_{\langle rr' \rangle} \vec{S}_r \cdot \vec{S}_{r'} + J_4 \sum_{\square} (P_{1234} + \text{H.c.}) = J_2 \widetilde{H}_2 + J_4 \widetilde{H}_4. \quad (1)$$

Here \vec{S}_r are spin-1/2 operators at the sites of a triangular lattice. The second term sums over all elementary parallelograms and P_{1234} performs a cyclic exchange of the four spins at the sites of the parallelogram. The multiple ring exchange is expected to be significant due to the proximity to the Mott transition in the organics. It is known that the three sublattice Neel order vanishes beyond a critical $J_4/J_2 \approx 0.1$ (Ref. 11) that can lead to novel spin-liquid phases with no long-range spin order.

We study various paired spin-liquid states for the J_2 - J_4 model using variational Monte Carlo calculations. In terms of wave functions, paired states may be described by Gutzwiller projected BCS states. Two natural states (which retain the full symmetry of the triangular lattice) are projected singlet $d_{x^2-y^2} + id_{xy}$ and nodal triplet $f_{x^3-3xy^2}$ wave

states. Remarkably in a range of J_4/J_2 with both J_2, J_4 antiferromagnetic we find that a projected singlet $d_{x^2-y^2}$ state has better energy than either of these states. The $d_{x^2-y^2}$ state is a gapless Z_2 spin-liquid state with nodal fermionic spinons and gapped Z_2 vortices (visons). In addition it *spontaneously* breaks the discrete rotational symmetry of the triangular lattice but preserves lattice translational symmetry. Thus, it is a gapless Z_2 spin liquid coexisting with a “nematic” or orientational order parameter. The pairing structure of the spinons determines the pairing structure of the superconductor that forms under pressure. Thus we propose a nodal d -wave state for the pressure-induced superconductor as well. Due to the discrete broken rotational symmetry, both the insulator and the superconductor will have nontrivial finite-temperature phase transitions in an ideal sample. We describe these and comment on their implications for the experiments.

We also study the J_2 - J_4 Hamiltonian for ferromagnetic J_2 while keeping the J_4 antiferromagnetic. In this case we find that of all the states studied, the triplet $f_{x^3-3xy^2}$ wave state has the minimum energy for a large range of J_4/J_2 . This result may have implications for the gapless spin-liquid behavior observed in 2D He-3 films.¹²

B. Relation to earlier work

Previous studies on the above model used a Gutzwiller projected filled Fermi sea to interpret the experiments.¹⁰ The low-energy theory of this state is described by a gapless Fermi surface of neutral spin-1/2 fermionic spinons coupled to a massless $U(1)$ gauge field (also obtained¹³ within a Hubbard model description). Reference 10 concluded that such a state is indeed the minimum-energy state for the J_2 - J_4 Hamiltonian for $J_4/J_2 \geq 0.30$ but the results were not conclusive for smaller values of J_4/J_2 . In particular, Ref. 10 found that many different projected BCS states in this regime have competitive energies making it difficult to pinpoint the true ground state. One of our goals is to resolve this ambiguity regarding the paired state. Theoretically, projected BCS states result as a condensation of the spinon pairs that gaps out the $U(1)$ gauge field and the resulting state is described as a Z_2 spin liquid. As was pointed out in Ref. 14, such states could explain a sharp crossover observed at $T \sim 5$ K in the experiments that could be associated with “pairing” of spinons. Reference 14 suggested an exotic paired state that retains a finite gapless portion of the spinon Fermi surface. The possibility of a more conventional triplet paired Z_2 state induced by Kohn-Luttinger effects¹⁵ of the spinons has also been pointed out.

Earlier numerical studies on the Hubbard model have also shed light on the zero-temperature phase diagram of half-filled triangular lattice.^{16–18} Of course, our model Hamiltonian [Eq. (1)] could be thought of as a low-energy limit of a Hubbard model in the insulating regime where we have allowed virtual charge fluctuations up to four-particle exchange. Using a variational wave-function approach, Ref. 17 did not find any evidence for a spin-liquid state and concluded that the insulating regime of the phase diagram is always magnetically ordered. Instead Refs. 16 and 18, using different variational wave functions, found evidence for a

projected nodal d -wave function in the insulating regime in agreement with our result for the ring-exchange Hamiltonian. Though it is not obvious to us which of these studies^{16–18} describe the correct ground state of the half-filled triangular lattice Hubbard model, it is desirable that a theoretical description of the organic salts κ CN or DMIT be consistent with the lack of any apparent order in the insulating regime apart, apart from being able to address other unusual properties mentioned above. We show in this paper that the projected nodal d -wave spin-liquid state successfully captures many of these features. Since ours is a pure spin model, a direct comparison of the ground-state energy with that obtained from variational studies on Hubbard model is not possible.

C. Outline

The paper is organized as follows. In Sec. II we describe the various variational paired spin-liquid states considered in our study along with a brief description of the method of optimization for these variational states. In Sec. III we describe the results. In particular, we show that the projected nodal $d_{x^2-y^2}$ state has the minimum energy of all the states considered. In Sec. IV we discuss the consequences and predictions of this result in the light of experimental work on organic superconductors. Section V considers the finite-temperature phase diagram for the nodal d -wave superconductor and corresponding projected spin liquid. We conclude with summary and discussion in Sec. VI.

II. VARIATIONAL WAVE FUNCTIONS

Various variational states may be constructed by starting with a system of spin-1/2 fermionic spinons $f_{r\alpha}$ hopping on a finite triangular lattice of size $L1 \times L2$ at half filling with a “mean-field” Hamiltonian,

$$H_{MF} = \sum_{rr'} [-t_{rr'} f_{r\alpha}^\dagger f_{r'\sigma} + (\Delta_{rr'} f_{r\uparrow}^\dagger f_{r'\downarrow}^\dagger + \text{H.c.})]. \quad (2)$$

The variational spin-wave function $|\Psi\rangle_{var} = P_G |\Psi\rangle_{MF}$, where the Gutzwiller projector $P_G = \prod_i (1 - n_{i\uparrow} n_{i\downarrow})$ ensures exactly one spinon per site. Unknown parameters in $|\Psi\rangle_{var}$ are fixed by minimizing the energy $E_{var} = \langle \Psi_{var} | H | \Psi_{var} \rangle / \langle \Psi_{var} | \Psi_{var} \rangle$ [with H given by Eq. (1)] with only nearest neighbor $t_{rr'} = t$. The simplest $|\Psi\rangle_{MF}$ corresponds to $\Delta_{rr'} = 0$, i.e., a filled Fermi sea. The corresponding $|\Psi\rangle_{var} \equiv |\Psi\rangle_{PFL} = P_G (\prod_{\vec{k}\sigma} f_{\vec{k}\sigma}^\dagger) |0\rangle$ with no variational parameters. The prime on the product implies restriction to \vec{k} such that the single-spinon level $\epsilon_{\vec{k}} \leq E_f$, the Fermi energy. More complex variational wave functions are obtained with different patterns of nonzero $\Delta_{rr'}$ which correspond to various projected BCS wave functions $|\Psi\rangle_{PBCS} = P_G |\text{BCS}\rangle = P_G (\sum_{\vec{k}} \phi_{\vec{k}} f_{\vec{k}\uparrow}^\dagger f_{-\vec{k}\downarrow}^\dagger)^{N/2} |0\rangle$. Here $\phi_{\vec{k}} = \Delta_{\vec{k}} / [\xi_{\vec{k}} + \sqrt{\xi_{\vec{k}}^2 + |\Delta_{\vec{k}}|^2}]$ with $\xi_{\vec{k}} = \epsilon_{\vec{k}} - \mu$. Further we write $\Delta_{\vec{k}}$, the Fourier transform of $\Delta_{rr'}$, as $\Delta_{\vec{k}} = \Delta_0 F(\vec{k})$, where the form of $F(\vec{k})$ is fully determined from a particular pattern of $\Delta_{rr'}$ (or equivalently, a particular Cooper-pair channel). The two variational parameters: gap parameter Δ_0 and the “chemical potential” μ are both deter-

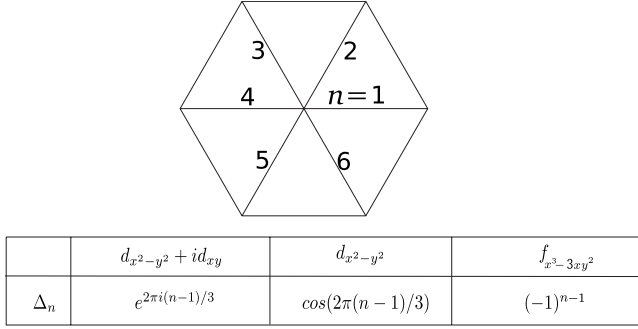


FIG. 1. Angular dependence of superconducting order parameter for the $d_{x^2-y^2}$, $d_{x^2-y^2} + id_{xy}$, and $f_{x^3-3xy^2}$ states.

mined by minimizing the energy. The minimization is done as follows. We first calculate the expectation value of the two-particle exchange term \widetilde{H}_2 and the four-particle exchange term \widetilde{H}_4 in Eq. (1) *separately* for a discrete set of values (μ_n, Δ_{0n}) such that $\mu_{min} < \mu_n < \mu_{max}$, $\Delta_{min} < \Delta_{0n} < \Delta_{max}$. The ranges for $\mu_{min/max}, \Delta_{0min/max}$ are chosen based on a preliminary minimization of the energy E_{var} such that the optimum values $\bar{\mu}, \bar{\Delta}_0$ lie within this range for *all* value of J_4/J_2 we are interested in. Having obtained the discretized functions $\widetilde{H}_2(\mu_n, \Delta_{0n})$ and $\widetilde{H}_4(\mu_n, \Delta_{0n})$, the optimization for any particular value of J_4/J_2 is achieved by simply picking the minimum of the function $J_2\widetilde{H}_2(\mu_n, \Delta_{0n}) + J_4\widetilde{H}_4(\mu_n, \Delta_{0n})$.

The properties of the three superconducting gap functions are as follows: the $d_{x^2-y^2} + id_{xy}$ state is invariant under spin rotation, lattice rotation, and translation symmetries, but breaks both time reversal and parity. After projection it corresponds to the ‘‘chiral spin-liquid’’ state.¹⁹ The $d_{x^2-y^2}$ state is a spin singlet with a $\cos(2\theta)$ angular dependence (θ is the angle subtended by a bond). It breaks lattice rotational symmetry while preserving translations and time reversal. Finally, the triplet $f_{x^3-3xy^2}$ -wave state has orbital part varying as $\cos(3\theta)$ while in spin space it has zero projection along a quantization axis. This breaks spin rotation but preserves all

the lattice symmetries and time reversal. Both $d_{x^2-y^2}$ and $f_{x^3-3xy^2}$ possess nodes along the Fermi surface in k space while $d_{x^2-y^2} + id_{xy}$ is fully gapped. Figure 1 shows the angular dependence of the SC gap $\Delta_{rr'}$ corresponding these three states on the triangular lattice.

III. RESULTS

A. Antiferromagnetic J_2

Figure 2(a) shows the difference $\delta E = E_{\text{PBCS}} - E_{\text{PFL}}$ for the three paired states, namely, projected $d_{x^2-y^2} + id_{xy}$, $f_{x^3-3xy^2}$, and $d_{x^2-y^2}$. Clearly for $J_4/J_2 \gtrsim 0.25$ the projected Fermi liquid (PFL) is the best variational state. Interestingly, for a wide range of parameters $0.10 \leq J_4/J_2 \leq 0.23$ the projected $d_{x^2-y^2}$ wins over the projected Fermi liquid as well as the other two paired states. In the regime, $0.23 \leq J_4/J_2 \leq 0.25$, the error bars preclude any conclusion. Figure 2(b) shows the optimal value of the gap parameter Δ_0 for these three states. Consistent with the results for optimal energy, $\Delta_0 \approx 0$ for $J_4/J_2 \gtrsim 0.25$ while for $0.10 \leq J_4/J_2 \leq 0.23$ the state $d_{x^2-y^2}$ has a nonzero and largest value of Δ_0 among all paired states. For smaller values of J_4/J_2 (≤ 0.10), it is expected that the spin-rotation symmetry-breaking spiral state would be the ground state of H .¹¹ In addition, we also studied a projected Fermi liquid with staggered flux Φ through alternate triangular plaquettes. We found that the energy has minima at $\Phi = 0, \pi$ and that the 0 flux state $|\Psi\rangle_{\text{PFL}}$ is always lower in energy than the π flux state for all values of J_4/J_2 .

Heuristically, large values of J_4/J_2 favors delocalization of electrons. Thus, it is not surprising that PFL is the ground state for large J_4/J_2 . Since $J_2 > 0$, the triplet paired f -wave state is expected to be unfavorable, consistent with our results. Further, the electrons are more delocalized in the nodal $d_{x^2-y^2}$ compared to $d_{x^2-y^2} + id_{xy}$ since the latter is fully gapped. Thus for values of J_4/J_2 not so small as to induce spiral order for spins but small enough that PFL is destabilized, our result that a projected nodal paired state is favored seems reasonable. Our results connect well with earlier

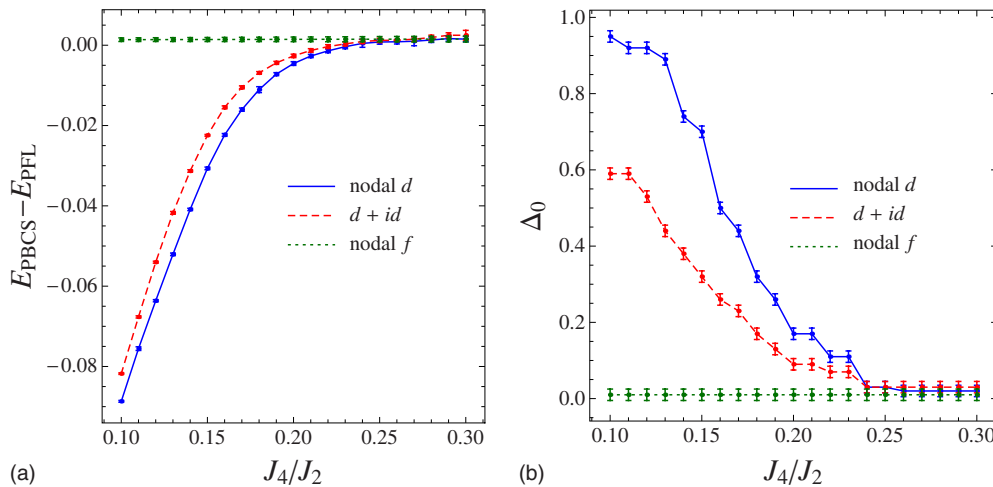


FIG. 2. (Color online) (a) Difference between E_{PBCS} and E_{PFL} for various paired states in the units of J_2 . The calculations are done on a 10×11 lattice with antiperiodic boundary conditions using the standard METROPOLIS Monte Carlo (Ref. 21) with 10^5 sweeps. (b) Gap parameter Δ_0 for various paired states in units of t .

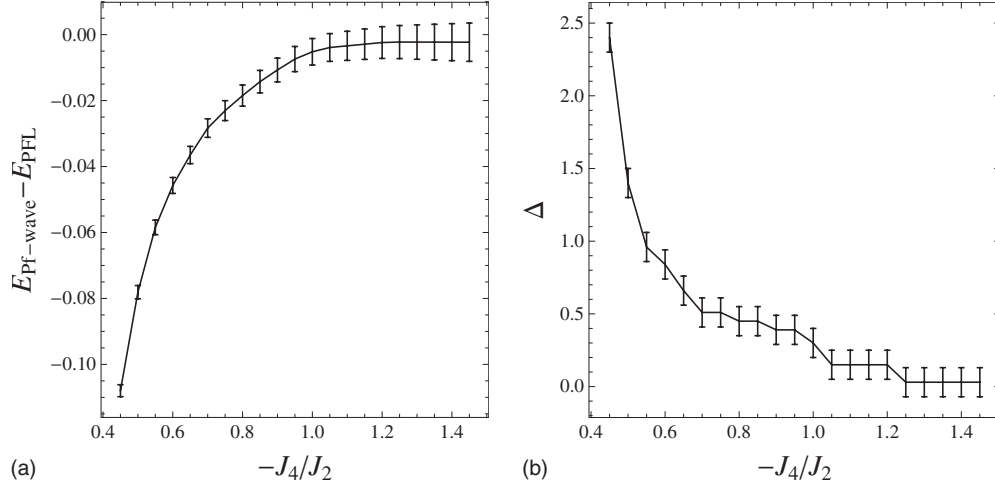


FIG. 3. (a) Difference between $E_{Pf-wave}$ and E_{PFL} as a function of J_4/J_2 for ferromagnetic J_2 . Both projected nodal d and $d+id$ have optimal value of $\Delta_0=0$ for this sign of J_2 and hence are not favorable compared to PFL. (b) Gap parameter Δ_0 for projected nodal f wave as a function of J_4/J_2 .

variational Monte Carlo¹⁶ and other numerical studies²⁰ of superconducting states in *anisotropic* triangular lattice Hubbard models which also found good evidence for a nodal d -wave state.

B. Ferromagnetic J_2

We also analyze the zero-temperature phase diagram for *ferromagnetic* J_2 (Fig. 3). Clearly at $J_4=0$, $J_2 < 0$, one obtains a fully polarized ferromagnet. For any $J_4 > 0$, expectedly we found that the spin-triplet projected nodal f -wave state is favored over the spin-singlet projected nodal d -wave and $d+id$ states. The projected f -wave state becomes favorable also compared to the ferromagnet for $J_4/J_2 \geq 0.40$. Finally for $J_4/J_2 \geq 1.5$, we find that the optimal value of $\Delta \approx 0$ for the projected f -wave state and thus the PFL state has the lowest energy. This is not very surprising since for $-J_4/J_2 \gg 1$, the sign of J_2 should not matter and thus the result is same as that for the antiferromagnetic J_2 case. Overall, the projected nodal f -wave state has the lowest energy of all the states considered (ferromagnet and the projected $d, d+id, f, FL$ states) for $1.5 \geq J_4/J_2 \geq 0.4$.

Under what circumstances is the ferromagnetic J_2 ring-exchange model relevant? Technically, a three-particle ring-exchange term with strength $J_3 (> 0)$ contributes ferromagnetically to the two-particle exchange because its sole effect is the replacement $J_2 \rightarrow J_2 - 2J_3$. Thus for $J_3 > J_2/2$, one would obtain a ferromagnetic ring-exchange model. However, a derivation of the ring-exchange Hamiltonian starting from the Hubbard model with only onsite repulsion has $J_n = 0$ for n odd irrespective of the underlying lattice. Since the organic salts κCN or DMIT are believed to be well described by the Hubbard model, we believe that the ferromagnetic model is not relevant to their physics. On the other hand, as shown by Ceperley and Jacucci,²² J_3 is indeed nonzero and bigger than $J_2/2$. Therefore, our results for ferromagnetic J_2 ring-exchange model may have implications for the observed spin-liquid behavior in two-dimensional He-3 films.¹² Further investigation in this direction would be desirable.

IV. PREDICTIONS AND COMPARISON WITH EXPERIMENTS

We now describe various properties of the state described by the nodal d -wave paired wave function. A mean-field Hamiltonian that describes the excitations of this state is simply the H_{MF} of Eq. (2). Fluctuations about the mean-field state are described by coupling the spinons to a Z_2 gauge field. This state is thus an example of a Z_2 spin liquid. The excitations of the Z_2 gauge field are Z_2 flux configurations (known as visons) which are gapped in this spin-liquid phase. The low-energy physics is then correctly described by the BCS Hamiltonian H_{MF} . Many properties of the nodal d -wave spin liquid at low temperature are thus similar to the familiar *spin* physics of a nodal d -wave superconductor. We now describe some of these in relation to the experiments.

Specific heat and spin susceptibility. In the absence of impurities, the density of states for a nodal superfluid vanishes linearly with energy and consequently the specific heat $C = aT^2$, where the coefficient a is, in principle, determined by the velocities that characterize the nodal dispersion of the spinons. Impurity scattering generates a nonzero density of states leading to a specific heat $C \sim \gamma T$ and a constant spin susceptibility χ_0 as $T \rightarrow 0$. Further, the low- T Wilson ratio $\chi T/C$ is constant of order 1. All of these are in agreement with the experiments on the organic spin-liquid materials.

The impurity-scattering rate can be roughly estimated by equating the entropies of the paired nodal spin-liquid and “normal” states at T^* , where T^* is a mean-field or crossover scale below which the pairing sets in (Fig. 4). Above T^* spinons may be described as having a gapless Fermi surface with a specific heat $C = \gamma_{spinon} T$. Here $\gamma_{spinon} = (\pi^2/3) k_B^2 n_{spinon}(E_f)$ and $n_{spinon}(E_f) = 0.28/t_{spinon}$ is the spinon density of states at the Fermi energy. Equating the entropies of the paired and normal states at T^* , we estimate $a = 2\gamma_{spinon}/T^*$. Impurities will cutoff the T^2 specific heat of the nodal spin liquid at a scale Γ and lead to a low- T gamma coefficient given by $\gamma = a\Gamma/k_B = 2\gamma_{spinon}\Gamma/(k_B T^*)$. Now $t_{spinon} \lesssim 2J_2 \approx 250$ K and from the measured low- T specific

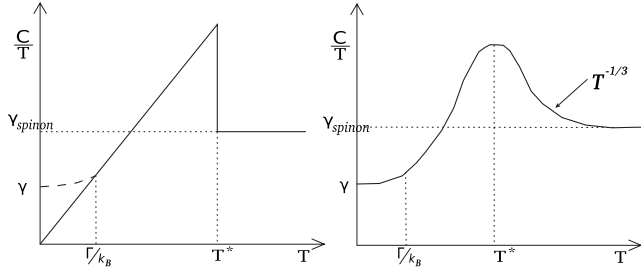


FIG. 4. Schematic sketch of the expected specific-heat curve. The left panel shows the mean-field behavior. The full line is in the clean limit and the dashed line the modification due to impurity scattering. The right panel shows the expected behavior when gauge fluctuations beyond mean field are included.

heat with $\gamma \approx 15 \text{ mJ K}^{-2} \text{ mol}^{-1}$, we estimate an impurity-scattering rate $\Gamma \leq 0.25 k_B T^* \approx 1.5 \text{ K}$. While Γ is reasonably small compared to superconducting gap it is appreciable enough to generate a constant density of states at low energy and lead to an apparent Fermi-liquidlike behavior in the specific heat at the lowest temperatures accessible, consistent with the experiments.⁴ The experiments also apparently show that the low-temperature linear specific heat is insensitive to magnetic fields up to about 8 T. This poses a difficulty for the present theory as the Zeeman coupling to the field is expected to increase the low-energy density of states. Indeed the prior proposal of an ‘‘Amperean’’ paired state¹⁴ was partly motivated by the insensitivity of the specific heat to a magnetic field. However as discussed below the Amperean pairing has some difficulty with describing the superconducting state that develops under pressure.

Thermal conductivity. Nodal spinons (as also dirty d -wave superconductors) lead to a finite ‘‘universal’’ metallic thermal conductivity $\kappa \sim T$ as $T \rightarrow 0$. In practice however observation of this effect requires low temperatures to eliminate the phonon contribution. In thermal transport measurements on κCN , a plot of κ/T as a function of T^2 of data above 1 K indeed extrapolates to a constant in the zero-temperature limit. However, data for $T \leq 0.5 \text{ K}$ rapidly extrapolates to zero and has been interpreted as evidence for a gap.²³ We do not have an explanation of this phenomenon.

Field induced inhomogeneity. At ambient pressure, NMR studies of κCN show the development of a magnetic-field induced inhomogeneity.³ Within our theory this may be rationalized as follows. Due to the effect proposed by Motrunich,²⁴ the external magnetic field induces an internal magnetic field for the spinons which can lead to vortices (visons) of the spinon pair condensate. The resulting ‘‘mixed state’’ is inhomogeneous that occurs below the pairing scale and increases in proportion to the field.

$T=0$ phase diagram under pressure and superconductivity. In general, pressure increases the ratio t/U , which implies an increase in J_4/J_2 leading to suppression of the pair amplitude. Thus increasing pressure suppresses the pairing transition. Increasing pressure also leads to an insulator-to-metal transition. Clearly two situations are possible depending on whether the pair order is killed before or after this metal-insulator transition. In the latter case superconductivity will be obtained in the metal close to the Mott phase bound-

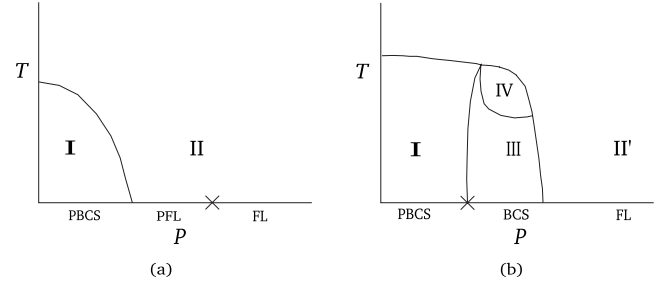


FIG. 5. Schematic pressure-temperature phase diagram for the nodal d -wave state. Figure (a)/(b) corresponds to the case when the pair order is killed before/after the Mott transition (denoted by ‘‘ \times ’’). Phase I corresponds to the finite-temperature threefold symmetry-breaking nematic insulator. The details of the regions II and II’ are determined by the nature of the Mott transition and/or finite- T crossover phenomena associated with the FL/PFL. We do not discuss it in this paper (please see Ref. 26 for a theory of region II). The phase III has long-range nematic order and power-law superconducting order while in the region IV both these orders have only power-law correlations. Please see the text for discussion of the associated phase transitions.

ary. We propose that this is realized in κCN . On the other hand, superconductivity has not been found in DMIT under pressure. We suggest that in this material the pair order is killed under pressure before the metal-insulator transition. An interesting experimental test of this suggestion is to study the Mott insulating phase of DMIT at pressures just below the metal-insulator phase boundary. Here the spinon Fermi-surface state, with its characteristic signatures such as, for instance, the $T^{2/3}$ heat capacity (produced by gauge fluctuations) will then survive to low T without any pairing transition.

If the pairing extends into the metallic phase the superconductor that results will also have $d_{x^2-y^2}$ symmetry and will (for an ideal isotropic triangular lattice) break lattice rotational symmetry. The spinons of the insulator now become the nodal Bogoliubov quasiparticles of this d -wave superconductor. Thus, the low-temperature specific heat and spin susceptibilities of the superconductor will behave similarly to that of the spin-liquid insulator. Further the NMR relaxation rate $1/T_1 T \sim T^2$ for $T > \Gamma$ (the impurity-scattering rate) and will saturate to a constant at the lowest temperatures. The former is in agreement with existing data on κCN for T close to T_c .⁵ Such a relaxation rate is not expected within the alternate Amperean paired state,¹⁴ making it difficult to connect the pairing transition in the spin liquid with that in the metal. The NMR data⁵ also shows that the Knight shift is only weakly suppressed on entering the superconducting state. However this may be due to complications associated with sample heating.²⁵

V. FINITE- T PHASE DIAGRAM

For an ideal isotropic triangular lattice the broken discrete rotational symmetry of the nodal d -wave state leads to an interesting finite-temperature phase diagram as shown in Fig. 5. Let the pairing field $\Delta_{\vec{a}}(\vec{r}) = \langle c_{\vec{r}\uparrow} c_{\vec{r}+\vec{a}\downarrow} - c_{\vec{r}\downarrow} c_{\vec{r}+\vec{a}\uparrow} \rangle$ on the

bond along direction \hat{a} emanating out of the site \vec{r} . Denoting the angle between \hat{a} and the x axis by $\theta_{\hat{a}}$, the order parameter for the nematic superconductor may be written as

$$\Psi(\vec{r}) = \sum_{\hat{a}} \cos(2\theta_{\hat{a}} - \phi) \Delta_{\hat{a}}(\vec{r}), \quad (3)$$

where the angle ϕ describes the orientation of the strong bond of the pair and the sum is over the six possible bond orientations. Since the orientational order is preserved under the symmetry operation corresponding to lattice inversion, ϕ takes one of three discrete values $0, 2\pi/3, 4\pi$. Defining $\psi_+(\vec{r}) = \sum_{\hat{a}} e^{2i\theta_{\hat{a}}} \Delta_{\hat{a}}(\vec{r}) e^{-i\phi}$ and $\psi_-(\vec{r}) = \sum_{\hat{a}} e^{-2i\theta_{\hat{a}}} \Delta_{\hat{a}}(\vec{r}) e^{i\phi}$, we may write

$$\Psi = \psi_+ + \psi_-. \quad (4)$$

The fields ψ_{\pm} carry electric charge 2, spin 0, and transforms nontrivially under lattice and time-reversal symmetries. In terms of these new variables, the orientational order parameter is proportional to $\psi_+^* \psi_-$. In describing the finite- T phase transition it will be convenient to allow ϕ to vary continuously and to impose the discreteness softly through an anisotropy term proportional to $(\psi_+^* \psi_-)^3 + c.c.$

First, consider the $d_{x^2-y^2}$ paired spin liquid that breaks the discrete orientational symmetry. In the spin liquid both ψ_{\pm} are coupled to a fictitious $U(1)$ gauge field \vec{a} with gauge charge two. In a phase-only description, one may write $\psi_+ = e^{i\theta_1}$, $\psi_- = e^{i\theta_2}$. A Landau expansion for the free energy F_I consistent with all the symmetries is readily written down in terms of θ_1, θ_2 as

$$\begin{aligned} F_I = & \int d^2x \cos(\vec{\nabla} \theta_1 - 2\vec{a}) + \cos(\vec{\nabla} \theta_2 - 2\vec{a}) \\ & + v \cos[3(\theta_1 - \theta_2)] + u \cos(\nabla \theta_1 - 2a) \cos(\nabla \theta_2 - 2a) \\ & + (\vec{\nabla} \times \vec{a})^2. \end{aligned} \quad (5)$$

Choosing the gauge $\theta_2=0$, one finds that the above expression for F_I corresponds to an XY model with threefold anisotropy for the field θ_1 . It is known that the critical behavior of this model corresponding to the ordering transition lies in the three-state Potts universality class. Thus as the temperature is increased, the insulating nematic phase undergoes a phase transition in the three-state Potts universality class at a certain temperature, say, T_{c1} . This corresponds to the phase boundary between phase I and II' in Fig. 5(b).

The nematic order also leads to a richer finite- T phase diagram in the superconductor. The crucial difference is that now there is no internal gauge field coupled to ψ_{\pm} . Thus in the absence of an external electromagnetic field, the Landau free energy F_{SC} may be written as

$$\begin{aligned} F_{SC} = & \int d^2x \cos(\nabla \theta_1) + \cos(\nabla \theta_2) + v \cos[3(\theta_1 - \theta_2)] \\ & + u \cos(\nabla \theta_1) \cos(\nabla \theta_2). \end{aligned} \quad (6)$$

Clearly at temperatures higher than all the energy scales that appear in F_{SC} , both θ_1 and θ_2 would be disordered. As the temperature is reduced coherence in θ_1, θ_2 would start to develop at a certain temperature, say, T_{c2} [which corresponds

to the line separating phase II' and IV in Fig. 5(b)]. Let us show that for small u, v , both θ_1, θ_2 undergo Kosterlitz-Thouless (KT) transitions into a sliding phase at T_{c2} . For this to happen, both u and v must be irrelevant at the KT critical point. As is readily checked, at the KT fixed point for the decoupled independent variables θ_1, θ_2 , the scaling dimension of v equals 2.25 while that of u is 4.0. Thus both these terms are indeed irrelevant at this fixed point and one concludes that the phase transition is indeed in the 2D XY universality class for both θ_1 and θ_2 .

As the temperature is reduced further, the variable $\theta_1 - \theta_2$, which corresponds to the orientational order parameter develops long-range order at some temperature T_{c3} , denoted by the line separating the phase III and IV in Fig. 5(b). To see this, let us introduce the variables $\tilde{\theta} = (\theta_1 + \theta_2)/2$, $\tilde{\phi} = (\theta_2 - \theta_1)/2$. In terms of these new variables, the free energy is

$$\begin{aligned} F_{SC} = & \int d^2x 2 \cos(\nabla \tilde{\phi}) \cos(\nabla \tilde{\theta}) + v \cos(6\tilde{\phi}) \\ & + u/2 [\cos(2 \nabla \tilde{\phi}) + \cos(2 \nabla \tilde{\theta})]. \end{aligned} \quad (7)$$

From this one concludes that the action consists of 2D XY model for $\tilde{\phi}$ with a sixfold anisotropy term that is known to be irrelevant at the KT fixed point. Thus we conclude that the phase transition for the orientational order parameter at the temperature T_{c3} lies in the *inverted* KT universality class. Note that the phase transition is inverted because the field $\tilde{\phi}$ has power-law correlations for $T_{c2} > T > T_{c3}$ while its connected component $\tilde{\phi} - \langle \tilde{\phi} \rangle$ has exponentially decaying correlations for $T < T_{c3}$. Thus both transitions at T_{c2} and T_{c3} are in the KT universality class with very weak signatures in the specific heat. However in both the insulator and the superconductor for the initial pairing transition, by the usual Ginzburg criterion, the fluctuation regime will be rather small. In practice, there is a small lattice anisotropy in both κ CN and DMIT, which will pin the nematic order parameter and smoothen out any sharp finite-temperature nematic transition. Further even in an isotropic material weak disorder acts as a ‘‘random field’’ on the nematic order parameter and will kill the finite-temperature nematic phase transition. Nevertheless if the disorder and the lattice anisotropy are weak, a sharp crossover behavior associated with the paired nematic order might be expected in the insulator. Such a crossover is visible in the existing experiments in a variety of properties. In this context we note that recent *ab initio* calculations^{27,28} find an anisotropy $t'/t \sim 0.8$ for κ CN. Here the hopping matrix element t corresponds to the parallel bonds of an elementary rhombus on the triangular lattice while t' corresponds to the diagonal bond. Since such an anisotropy would make the lattice symmetry closer to that of a square lattice, physical reasoning as well as the results from papers^{16,18} imply that the nodal $d_{x^2-y^2}$ becomes even more stable for the actual material.

VI. SUMMARY AND DISCUSSION

To summarize we studied the energetics of various Gutzwiller projected BCS states for the triangular lattice an-

tiferromagnet with a four-particle ring exchange. In a range of parameters the best state is a projected $d_{x^2-y^2}$ paired state which breaks lattice rotational symmetry. We described many properties of this state that can account for a number of measured properties of the organic materials. The most serious difficulty at present is the field independence of the specific heat. Perhaps the impurity-scattering rate Γ can be bigger than our rough estimate without any major effect on the pairing transition temperature.

Are there any “smoking gun” tests of our proposal for future experiments? The essence of our proposed gapless Z_2 spin-liquid state can be probed in experiments on κ CN through the flux trapping effect described in Ref. 29. We note that such experiments have been performed on the cuprate materials³⁰ and may be feasible in the organics as well. A Josephson tunneling experiment with a spin-liquid insulating barrier between two superconductors has also been proposed as a probe of the gapped charge- e spin-0 charge carriers expected in this spin-liquid state.³¹ Future experiments will hopefully shed light on whether such a paired nematic spin liquid really exists in these materials.

We also studied the model with ferromagnetic Heisenberg exchange J_2 and antiferromagnetic ring exchange J_4 and found that among the projected BCS/Fermi-liquid spin-liquid states, the projected nodal f -wave state has minimum energy for wide range of values of J_4/J_2 .

Finally, we studied the finite-temperature phase diagram for the nodal d -wave state and found that for an isotropic triangular lattice one would encounter interesting phases and phase transitions as one changes temperature. In particular, there is a possibility of a sliding phase with power-law correlations for both superconducting and orientational order parameters.

ACKNOWLEDGMENTS

We thank K. Kanoda, O. Motrunich, and Y. Ran for helpful discussions. T.S. was supported by NSF under Grant No. DMR-0705255, N.T. by DOE under Grant No. DE-FG02-07ER46423 and PAL by NSF under Grant No. DMR-0804040.

-
- ¹Y. Shimizu, K. Miyagawa, K. Kanoda, M. Maesato, and G. Saito, *Phys. Rev. Lett.* **91**, 107001 (2003).
- ²Y. Kurosaki, Y. Shimizu, K. Miyagawa, K. Kanoda, and G. Saito, *Phys. Rev. Lett.* **95**, 177001 (2005).
- ³Y. Shimizu, K. Miyagawa, K. Kanoda, M. Maesato, and G. Saito, *Phys. Rev. B* **73**, 140407(R) (2006).
- ⁴S. Yamashita, Y. Nakazawa, M. Oguni, Y. Oshima, H. Nojiri, Y. Shimizu, K. Miyagawa, and K. Kanoda, *Nat. Phys.* **4**, 459 (2008).
- ⁵Y. Shimizu, H. Kasahara, T. Furuta, K. Miyagawa, K. Kanoda, M. Maesato, and G. Saito, *Phys. Rev. B* **81**, 224508 (2010).
- ⁶T. Itou, A. Oyamada, S. Maegawa, M. Tamura, and R. Kato, *J. Phys.: Condens. Matter* **19**, 145247 (2007).
- ⁷T. Itou, A. Oyamada, S. Maegawa, M. Tamura, and R. Kato, *Phys. Rev. B* **77**, 104413 (2008).
- ⁸T. Itou, A. Oyamada, S. Maegawa, M. Tamura, and R. Kato, *J. Phys.: Conf. Ser.* **145**, 012039 (2009).
- ⁹P. W. Anderson, *Mater. Res. Bull.* **8**, 153 (1973).
- ¹⁰O. I. Motrunich, *Phys. Rev. B* **72**, 045105 (2005).
- ¹¹W. LiMing, G. Misguich, P. Sindzingre, and C. Lhuillier, *Phys. Rev. B* **62**, 6372 (2000).
- ¹²R. Masutomi, Y. Karaki, and H. Ishimoto, *Phys. Rev. Lett.* **92**, 025301 (2004).
- ¹³S.-S. Lee and P. A. Lee, *Phys. Rev. Lett.* **95**, 036403 (2005).
- ¹⁴S.-S. Lee, P. A. Lee, and T. Senthil, *Phys. Rev. Lett.* **98**, 067006 (2007).
- ¹⁵V. Galitski and Y. B. Kim, *Phys. Rev. Lett.* **99**, 266403 (2007).
- ¹⁶J. Liu, J. Schmalian, and N. Trivedi, *Phys. Rev. Lett.* **94**, 127003 (2005).
- ¹⁷T. Watanabe, H. Yokoyama, Y. Tanaka, and J. Inoue, *Phys. Rev. B* **77**, 214505 (2008).
- ¹⁸L. Tocchio, A. Parola, C. Gros, and F. Becca, *Phys. Rev. B* **80**, 064419 (2009).
- ¹⁹V. Kalmeyer and R. B. Laughlin, *Phys. Rev. Lett.* **59**, 2095 (1987); X.-G. Wen, F. Wilczek, and A. Zee, *Phys. Rev. B* **39**, 11413 (1989).
- ²⁰B. Kyung and A.-M. S. Tremblay, *Phys. Rev. Lett.* **97**, 046402 (2006).
- ²¹A. Paramekanti, M. Randeria, and N. Trivedi, *Phys. Rev. B* **70**, 054504 (2004); C. Gros, *Ann. Phys.* **189**, 53 (1989); D. M. Ceperley, G. V. Chester, and M. H. Kalos, *Phys. Rev. B* **16**, 3081 (1977).
- ²²D. M. Ceperley and G. Jacucci, *Phys. Rev. Lett.* **58**, 1648 (1987).
- ²³M. Yamashita, N. Nakata, Y. Kasahara, T. Sasaki, N. Yoneyama, N. Kobayashi, S. Fujimoto, T. Shibauchi, and Y. Matsuda, *Nat. Phys.* **5**, 44 (2009).
- ²⁴O. I. Motrunich, *Phys. Rev. B* **73**, 155115 (2006).
- ²⁵K. Kanoda (private communication).
- ²⁶T. Senthil, *Phys. Rev. B* **78**, 045109 (2008).
- ²⁷K. Nakamura, Y. Yoshimoto, T. Kosugi, R. Arita, and M. Imada, *J. Phys. Soc. Jpn.* **78**, 083710 (2009).
- ²⁸H. C. Kandpal, I. Opahle, Y.-Z. Zhang, H. O. Jeschke, and R. Valentí, *Phys. Rev. Lett.* **103**, 067004 (2009).
- ²⁹T. Senthil and M. P. A. Fisher, *Phys. Rev. Lett.* **86**, 292 (2001); *Phys. Rev. B* **63**, 134521 (2001).
- ³⁰D. A. Bonn, J. C. Wynn, B. W. Gardner, Y.-J. Lin, R. Liang, W. N. Hardy, J. R. Kirtley, and K. A. Moler, *Nature (London)* **414**, 887 (2001).
- ³¹T. Senthil and M. P. A. Fisher, *Phys. Rev. B* **64**, 214511 (2001).